Spatial-Temporal Mercer Kernel for Premature Ventricular Complex Estimation in Electrocardiographic Imaging

Enrique Feito-Casares[1], Francisco M Melgarejo-Meseguer[1],
Yeşim Serinağaoğlu-Doğrusöz[2], José Luis Rojo-Álvarez[1]

[1] Departamento de Teoría de la Señal y Comunicaciones y Sistemas Telemáticos y Computación. Universidad Rey Juan Carlos, Madrid, Spain.
[2] Electrical Electronics Engineering Department. Middle East Technical University, Turkey.

Abstract

Cardiovascular diseases are a leading cause of death globally, highlighting the need for accurate, noninvasive diagnostic tools. Electrocardiographic imaging (ECGI) has emerged as a promising technique for reconstructing epicardial potentials from body surface measurements, offering an alternative to invasive procedures. This work presents a novel spatio-temporal separable Mercer kernel framework for estimating premature ventricular complex (PVC) origins, aiming to enhance the precision of ECGI-based localization. We incorporate spatial-temporal correlations in the kernel and use ADAM optimization to model epicardial potential dynamics. The proposed approach is evaluated using real ECGI data, and its performance is compared to traditional methods, including the Tikhonov regularization. Results show that the Gaussian kernel achieves the lowest NSME (0.3439) and smallest localization error (12.55 mm), outperforming the Laplacian kernel (NSME = 0.3503; 23.99 mm) and Tikhonov (NSME = 0.5036; 36.48 mm). This study contributes to advancing ECGI as a reliable tool for guiding catheter ablation in PVC patients, improving clinical outcomes through previous localization.

1. Introduction

Cardiovascular diseases remain a leading cause of premature mortality worldwide, with 17.9 million lives lost each year, creating a constant demand for more accurate, efficient, and noninvasive diagnostic tools [1]. Traditional 12-lead electrocardiograms (ECG) are well established as the gold standard in electrocardiology and widely used due to their accessibility, but with insufficient spatial resolution. In contrast, invasive intracardiac mapping provides detailed insights at the cost of procedural complexity and patient risk. Electrocardiographic imaging (ECGI) has emerged as a noninvasive approach to map cardiac electrical activity from body surface potential measurements (BSPM) to epicardial potential source estimation [2].

Premature Ventricular Contractions (PVCs) are a frequent arrhythmic event, affecting 40% to 75% of the general population with varying prevalence with age and comorbidities [3]. For many years, it has been understood that benign symptomatic or high-burden PVCs can potentially lead to cardiomyopathy and provoke more severe arrhythmias. In such cases, catheter ablation has been recognized as the preferred treatment approach. However, the success of this procedure heavily relies on the precise identification of the PVC origin [4]. Recent studies have highlighted the potential of ECGI to improve the accuracy of PVC localization, thereby offering support for ablation planning [5].

This work proposes a novel spatial-temporal Mercer kernel framework and ADAM optimization for estimating PVC origins from ECGI data. Our approach seeks to improve the precision of inverse solutions by incorporating spatial and temporal correlations into the kernel design. The goal is to reduce localization error while maintaining robustness across varying patient anatomies and PVC origin sites. This contribution builds on our prior work and aims to move ECGI closer to becoming a reliable clinical tool for guiding catheter ablation in PVC patients.

2. Materials and Methods

We introduce the methods for modeling epicardial potentials based on spatio-temporal kernel modeling and the experimental dataset used, and the mathematical formulation of the ECGI inverse problem.

2.1. ECGI Inverse Problem

The ECGI inverse problem involves reconstructing epicardial potentials from body surface measurements. The extracellular potential is denoted as $v_e(\boldsymbol{r}_e, t)$, representing the torso potential in the context of the inverse elec-

trocardiography problem. The source potential is denoted as $v_s(\boldsymbol{r}_s, t)$, representing the epicardial potential, while the transmission operator is $H(\boldsymbol{r}_e, \boldsymbol{r}_s)$. The fundamental equation governing the relationship between these potentials is:

$$v_e(\boldsymbol{r}_e, t) = H(\boldsymbol{r}_e, \boldsymbol{r}_s) v_s(\boldsymbol{r}_s, t) \tag{1}$$

Here, $\boldsymbol{r}_e \in S_e$ and $\boldsymbol{r}_s \in S_s$ represent the continuous surfaces on which the measurements and sources are located, respectively. The discretization process occurs in time at $t = t_n = nT_s$, where $n = 1, \ldots, N_t$. The measurement surface S_e is discretized into a set of points $\boldsymbol{r}_e^i$ with $i = 1, \ldots, N_e$, while the source surface S_s is discretized into a set of points $\boldsymbol{r}_s^j$ with $j = 1, \ldots, N_s$. We can discretize in space and time as:

$$\boldsymbol{H}(i,j) = H(\boldsymbol{r}_e^i, \boldsymbol{r}_s^j), \tag{2}$$

$$\boldsymbol{V}_e(i,n) = v_e(\boldsymbol{r}_e^i, n\Delta t) \tag{3}$$

$$\boldsymbol{V}_s(j,n) = v_s(\boldsymbol{r}_s^j, n\Delta t) \tag{4}$$

so that $\boldsymbol{H} \in \mathbb{R}^{N_e \times N_s}$, $\boldsymbol{V}_e \in \mathbb{R}^{N_e \times N_t}$, $\boldsymbol{V}_s \in \mathbb{R}^{N_s \times N_t}$, and then, the matrix-form expression is

$$\boldsymbol{V}_e = \boldsymbol{H}\boldsymbol{V}_s \tag{5}$$

The solution is

$$\hat{\boldsymbol{V}}_s = \arg\min_{\boldsymbol{V_s}} \underbrace{\|\boldsymbol{V}_e - \boldsymbol{H}\boldsymbol{V}_s\|_2^2}_{\text{Data-fidelity term}} + \underbrace{\gamma \|\boldsymbol{L}\boldsymbol{V}_s\|_2^2}_{\text{Regularization term}} . \tag{6}$$

The data-fidelity term in the optimization problem penalizes the discrepancy between the measured torso potential $\boldsymbol{V}_e$ and the estimated epicardial potential $\boldsymbol{V}_s$, which is generated by the forward model $\boldsymbol{H}$. The regularization parameter γ controls the balance between the fit to the observed data and the enforcement of prior information, providing a trade-off between minimizing residual error and ensuring smoothness or other desired properties in the solution. The matrix $\boldsymbol{L}$ is the regularization operator, usually the identity matrix.

The Zero-order Tikhonov (ZOT) method is a popular technique for solving the inverse problem optimization in Eq. 6 by algebraic manipulation. In this particular case, a closed solution appears as:

$$\hat{\boldsymbol{V}}_s(\gamma) = \left(\boldsymbol{H}^\top \boldsymbol{H} + \gamma^2 \boldsymbol{L}^\top \boldsymbol{L}\right)^\dagger \boldsymbol{H}^\top \boldsymbol{V}_e, \tag{7}$$

where denotes the Moore-Penrose pseudoinverse. The ZOT model serves as a baseline for comparison with other proposed models.

2.2. Spatio-temporal Kernel Modeling

In ECGI, accurately reconstructing epicardial potentials from body surface measurements presents significant challenges. The primary difficulty lies in capturing the complex dynamics that emerge from the spatio-temporal nature of the epicardial potentials. To address this issue, we introduce a spatio-temporal kernel-based approach. This method leverages the separability between the spatial and temporal components of the kernel, enabling a more precise modeling of the source potential. In this setting, a time-space expansion of the source potential in S_s is given by

$$v_s(\boldsymbol{r}_s, t) \approx \sum_{n=1}^{N_t} \sum_{j=1}^{N_s} \alpha_{n,s} K(\boldsymbol{r}_s - \boldsymbol{r}_s^j, t - t_n) \tag{8}$$

where

$$K(\boldsymbol{r}, t) = e^{\left(-\frac{\|\boldsymbol{r}\|^2}{2\sigma_s^2}\right)} e^{\left(-\frac{|t|^2}{2\sigma_t^2}\right)} = K_s(\boldsymbol{r}) K_t(t) \tag{9}$$

is a Mercer kernel, and σ_s, σ_t are the kernel bandwidths for spatial sources and time. The spatio-temporal kernel is separable in time and space. We can discretize in space and time,

$$\boldsymbol{K}_s(j, j') = K_s(\boldsymbol{r}_s^j - \boldsymbol{r}_s^{j'}), \tag{10}$$

$$\boldsymbol{K}_t(n, n') = K_t(n - n'). \tag{11}$$

so that $\boldsymbol{K}_s \in \mathbb{R}^{N_s \times N_s}$ and $\boldsymbol{K}_t \in \mathbb{R}^{N_t \times N_t}$. Then, the matrix-form expression is:

$$\hat{\boldsymbol{V}}_e = \boldsymbol{H}\boldsymbol{V}_s \approx \boldsymbol{H}\boldsymbol{K}_s\boldsymbol{\alpha}\boldsymbol{K}_t \tag{12}$$

where $\boldsymbol{\alpha} \in \mathbb{R}^{N_s \times N_t}$, The functional to be minimized has the matrix form:

$$J(\boldsymbol{\alpha}) = \min_{\boldsymbol{\alpha}} \|\boldsymbol{E}(\boldsymbol{\alpha})\|_2^2 = \min_{\boldsymbol{\alpha}} \|\boldsymbol{V}_e - \boldsymbol{H}\boldsymbol{K}_s\boldsymbol{\alpha}\boldsymbol{K}_t\|_2^2 \tag{13}$$

In this setting, specific strategies must be considered to deal with the selection of hyperparameters of the kernel and the optimization algorithm for the spatio-temporal functional.

There are numerous approaches to regularizing the inverse problem in the literature. However, few sample studies implement cross-validation strategies to search for the free parameters [6]. An out-of-sample cross-validation strategy adapted from the one proposed in the previously cited work was used to search for the hyperparameters of $\boldsymbol{K}_s$ and $\boldsymbol{K}_t$.

2.3. Optimization

The optimization problem in Eq. (13) can be tackled using gradient descent, although there are no guarantees of reaching a global minimum, given the computed gradient

$$\nabla_{\boldsymbol{\alpha}} L(\boldsymbol{\alpha}) = \left(-\boldsymbol{K}_s^T \boldsymbol{H}^T \boldsymbol{E}(\boldsymbol{\alpha}) \boldsymbol{K}_t^T\right) \tag{14}$$

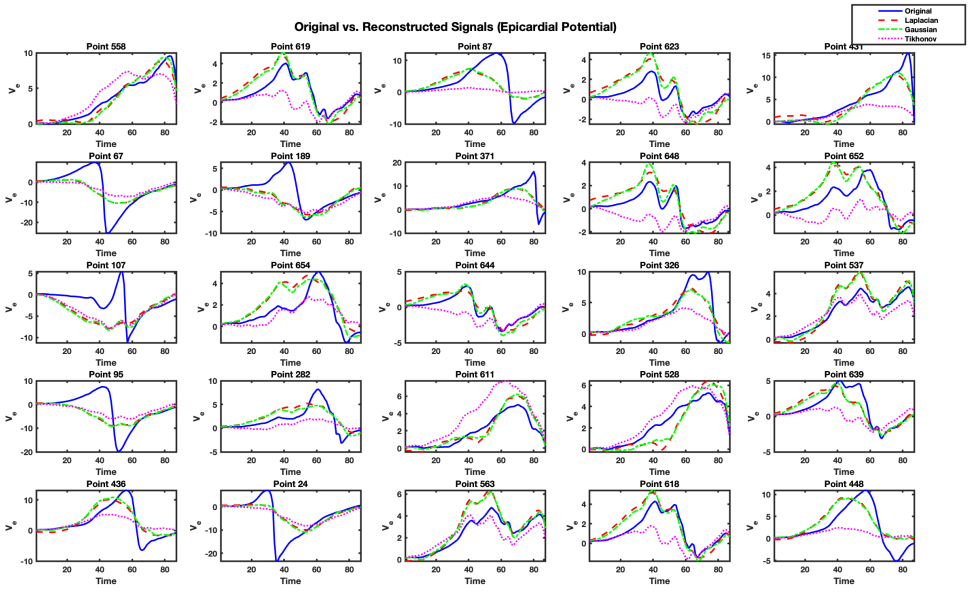

Figure 1. Comparison of original and reconstructed epicardial potential signals at various spatial points.

Gradient descent makes it feasible to compute the optimization variable matrix $\boldsymbol{\alpha}$, especially as the number of spatial and temporal samples increases. To overcome the limitations of traditional gradient descent, the Adam optimizer is widely recognized as an effective alternative in iterative gradient descent optimization [7].

2.4. Experimental Dataset

The experiments were developed using real bioelectric signals from the EDGAR Time Signal Catalog [8]. The first selected dataset was for the ischemia torso tank with a cardiac cage, obtained and publicly shared by Utah University [9]. This dataset consists of 4 subsets, namely a control subset plus three intervention subsets, each composed of several torso and cavity geometry records and a transfer matrix $\boldsymbol{H}$ with size 192×684. The torso signal recordings consisted of 192 signals from BSPM sensor signals, while the cavity records consisted of 684 needle sensor signals, which are known as electrograms, connected to the cage.

3. Experiments and Results

In this experiment, we evaluated the performance of three methods for reconstructing epicardial potential signals. The methods tested include the Tikhonov method, which serves as the baseline, and two spatio-temporal kernel methods, using Laplacian and Gaussian kernels. Hyperparameter tuning for each method was performed using a cross-validation strategy to optimize reconstruction accuracy.

The reconstruction accuracy of the electrograms was assessed using the Normalized Squared Mean Error (NSME), with the following results: the Laplacian kernel achieved an NSME of 0.3503, the Gaussian kernel had an NSME of 0.3439, and the Tikhonov method yielded the highest error with an NSME of 0.5036. Additionally, more quantitative metrics are assessed. Tikhonov yields a temporal correlation coefficient of 0.715 ± 0.270 (median ± IQR), a relative error of 0.724 ± 0.202, and the largest localization error (36.48 mm). The Gaussian kernel achieves the best performance, with 0.820 ± 0.199 correlation, 0.586 ± 0.244 relative error, and the smallest localization error (12.55 mm). The Laplacian kernel performs intermediately at 0.801 ± 0.192 correlation, 0.606 ± 0.245 relative error, and 23.99 mm localization error. These results show that the Gaussian kernel provides the most accurate reconstruction, closely followed by the Laplacian kernel.

Given the previous results, Figure 1 compares the original and reconstructed signals at several spatial points. The Tikhonov method shows more noticeable discrepancies from the original signal; these discrepancies are particularly pronounced in cases with a sudden change in potential. In some cases, the Gaussian and Laplacian kernel methods handle the estimation better, although they still produce biased results. Figure 2 compares activation time (AT) maps for the proposed methods. To compute the AT, the electrograms were first preprocessed using a 4th-order Butterworth band-pass filter (100 Hz to 1000 Hz), and then the activation times were estimated following the approach described in [10]. The Tikhonov method produces more smoothed patterns, with blurred activation fronts and significant displacement of the earliest activation site. This is

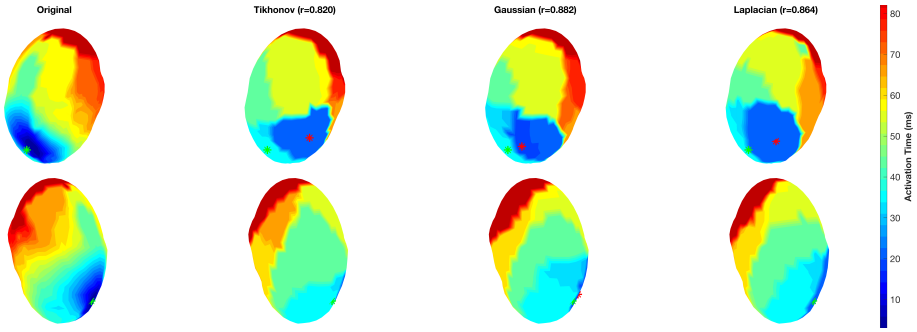

Figure 2. Activation time (AT) maps and the correlation coefficient (r) between reconstructed and original AT maps. Red and green asterisks denote the estimated and true earliest activation sites, respectively.

reflected in a lower correlation with the reference AT maps (r = 0.820), indicating reduced spatial fidelity. In contrast, the Gaussian kernel preserves sharper spatial gradients, achieves the highest correlation (r = 0.882), and aligns the earliest activation sites more closely with the ground truth. The Laplacian kernel also improves over Tikhonov, with a correlation of r = 0.864, though with slightly greater spatial diffusion than the Gaussian kernel.

4. Conclusions

This study evaluated three methods for reconstructing epicardial potential signals: the Tikhonov method, the Laplacian spatio-temporal kernel, and the Gaussian spatio-temporal kernel. The results show that both kernel-based methods, particularly the Gaussian kernel, outperform the Tikhonov method in terms of reconstruction accuracy. These preliminary findings highlight that spatio-temporal kernel-based approaches pose an encouraging direction for addressing the ECGI inverse problem. Future work may focus on optimizing kernel-measured spatio-temporal correlations.

Acknowledgments

This work was supported by the Research Grants HERMES, LATENTIA, AND PCardioTrials. (PID2023-152331OA-I00, PID2022-140786NB-C31, and PID2022-140553OA-C42), funded by MICIU/AEI/ 10.13039/ 501100011033. Also supported by Rey Juan Carlos University, project HERMES 2024/00004/00, and a grant from Comunidad de Madrid to the Madrid ELLIS Unit.

References

[1] World Health Organization. Fact sheet on cardiovascular diseases (CVDs).

[2] Cluitmans M, Brooks DH, MacLeod R, Dössel O, Guillem MS, Van Dam PM, Svehlikova J, He B, Sapp J, Wang L, Bear L. Validation and Opportunities of Electrocardiographic Imaging: From Technical Achievements to Clinical Applications. Frontiers in Physiology September 2018; 9:1305.

[3] Messineo FC. Ventricular ectopic activity: Prevalence and risk. The American Journal of Cardiology December 1989; 64(20):J53–J56.

[4] Enriquez A, Muser D, Markman TM, Garcia F. Mapping and Ablation of Premature Ventricular Complexes. JACC Clinical Electrophysiology June 2024;10(6):1206–1222.

[5] Sánchez J, Llorente-Lipe I, Espinosa CB, Loewe A, Hernández-Romero I, Vicente-Puig J, Ros S, Atienza F, Carta-Bergaz A, Climent AM, Guillem MS. Enhancing premature ventricular contraction localization through electrocardiographic imaging and cardiac digital twins. Computers in Biology and Medicine May 2025;190:109994.

[6] Melgarejo-Meseguer FM, Everss-Villalba E, Gutierrez-Fernandez-Calvillo M, Munoz-Romero S, Gimeno-Blanes FJ, Garcia-Alberola A, Rojo-Alvarez JL. Generalization and Regularization for Inverse Cardiac Estimators. IEEE Transactions on Biomedical Engineering October 2022; 69(10):3029–3038.

[7] Kingma DP, Ba J. Adam: A method for stochastic optimization. In Bengio Y, LeCun Y (eds.), 3rd International Conference on Learning Representations, ICLR. May 2015; 1–15.

[8] Aras K, Good W, Tate J, Burton B, Brooks D, Coll-Font J, Doessel O, Schulze W, Potyagaylo D, Wang L, Van Dam P, MacLeod R. Experimental Data and Geometric Analysis Repository—EDGAR. Journal of Electrocardiology November 2015;48(6):975–981.

[9] Tate J, Gillette K, Burton B, Good W, Zenger B, Coll-Font J, Brooks D, MacLeod R. Reducing Error in ECG Forward Simulations With Improved Source Sampling. Frontiers in Physiology September 2018;9:1304.

[10] Erem B, Coll-Font J, Martinez Orellana R, St'ovicek P, Brooks DH. Using Transmural Regularization and Dynamic Modeling for Noninvasive Cardiac Potential Imaging of Endocardial Pacing With Imprecise Thoracic Geometry. IEEE Transactions on Medical Imaging March 2014; 33(3):726–738. ISSN 0278-0062, 1558-254X.

Address for correspondence:

Enrique Feito-Casares. University Rey Juan Carlos, Fuenlabrada (Madrid), Spain. Mail to: enrique.feito@urjc.es